Optical preparation of H2 rovibrational levels with almost complete population transfer

Wenrui Dong, Nandini Mukherjee, and Richard N. Zare

Citation: J. Chem. Phys. **139**, 074204 (2013); doi: 10.1063/1.4818526
View online: http://dx.doi.org/10.1063/1.4818526
View Table of Contents: http://jcp.aip.org/resource/1/JCPSA6/v139/i7
Published by the AIP Publishing LLC.

Optical preparation of H_2 rovibrational levels with almost complete population transfer

Wenrui Dong,[a] Nandini Mukherjee,[a] and Richard N. Zare
Department of Chemistry, Stanford University, Stanford, California 94305-5080, USA

(Received 17 June 2013; accepted 17 July 2013; published online 20 August 2013)

Using stimulated Raman adiabatic passage (SARP), it is possible, in principle, to transfer all the population in a rovibrational level of an isolated diatomic molecule to an excited rovibrational level. We use an overlapping sequence of pump (532 nm) and dump (683 nm) single-mode laser pulses of unequal fluence to prepare isolated H_2 molecules in a molecular beam. In a first series of experiments we were able to transfer more than half the population to an excited rovibrational level [N. Mukherjee, W. R. Dong, J. A. Harrison, and R. N. Zare, J. Chem. Phys. **138**(5), 051101-1–051101-4 (2013)]. Since then, we have achieved almost complete transfer (97% ± 7%) of population from the H_2 ($v = 0, J = 0$) ground rovibrational level to the H_2 ($v = 1, J = 0$) excited rovibrational level. An explanation is presented of the SARP process and how these results are obtained. © *2013 AIP Publishing LLC*. [http://dx.doi.org/10.1063/1.4818526]

I. INTRODUCTION

In many experiments it is desirable to prepare molecular targets in pure quantum states. Various optical preparation schemes such as visible,[1] infrared,[2,3] or Raman pumping[4,5] are often used to meet this goal. However, many of these experiments are made difficult by the inability to transfer large populations to a desirable target quantum state. One way to overcome this problem is to transfer population between quantum states using adiabatic passage. Previously stimulated Raman adiabatic passage (STIRAP)[6–9] and Stark-chirped rapid adiabatic passage (SCRAP)[10–15] processes were utilized to transfer nearly the complete population between an initial and a target quantum state. However, for the purpose of transferring population between two rovibrational levels within the ground electronic surface of a molecule, both these techniques require a suitable resonant, or near resonant intermediate vibronic state connecting the initial and final (target) rovibrational levels. For H_2, and many other molecules having a wide energy band-gap between the ground and excited electronic states, STIRAP or SCRAP will require the use of vacuum ultraviolet (VUV) or extreme ultraviolet (XUV) pulses, making it a complicated system to realize in practice. Moreover, in the presence of an intermediate vibronic resonance, the short wavelength pulses with high peak powers may cause significant ionization or dissociation of the molecule. Another alternative for preparing vibrationally excited molecules is chirped adiabatic Raman passage (CARP)[16,17] which does not require an intermediate state. However, CARP does require high-energy picosecond laser pulses with the desirable chirping rate to fulfill the condition of adiabatic passage. Again, this technique poses practical difficulties to realize. We have previously proposed another alternative for achieving complete population transfer between two rovibrational levels, without requiring an intermediate vibronic resonance and without frequency chirping.[18,19] It is based on Stark-induced adiabatic Raman passage (SARP). SARP uses a sequence of partially overlapping off-resonant nanosecond pump and dump pulses of unequal intensities. The pulse with the higher intensity (pump or dump) generates the necessary sweep of the Raman resonance frequency by inducing second-order (dynamic) Stark shifts of the rovibrational levels. During the pulsed excitation the Raman transition frequency is swept through resonance twice. The delay between the pulses is adjusted so that significant Raman coupling (overlap of pump and dump pulses) can occur only at one of the crossings of the Raman resonance. To prevent the coherent population return, the other crossing must be passed with negligible Raman coupling. As the Raman resonance is crossed with sufficiently strong Raman coupling, a unidirectional flow of population from the initial to the final target state takes place during the overlap of the pump and dump pulses. Recently, we provided the first demonstration of SARP to pump H_2 in a molecular beam, but we were only able to achieve approximately 73% transfer.[20] This paper is an extension of this study in which we present new experimental data showing that SARP is able to achieve almost complete population transfer from the ground $H_2(v = 0, J = 0)$ to an excited rovibrational state $H_2(v = 1, J = 0)$, as predicted by the theory.

II. EXPERIMENTAL METHOD

Figure 1 shows a schematic of the SARP experiment. The second harmonic of a Nd:YAG laser (Continuum Lasers Inc.) was separated by a beam splitter (BS1). One portion (40%) is used as a pump pulse (single-mode 532 nm, 6 ns duration) for the SARP process on the H_2 molecules. The other portion (60%) is used to prepare the dump pulse (single-mode 683 nm, 4.6 ns duration). The latter comes from the output of a pulsed dye amplifier (PDA), which is seeded by a cw dye laser (Mattise DS), pumped with a cw diode-pumped Nd:YVO_4 laser (Millennia). The pump laser pulse after passing through an adjustable optical delay line spatially overlaps

[a]W. Dong and N. Mukherjee contributed equally to this work.

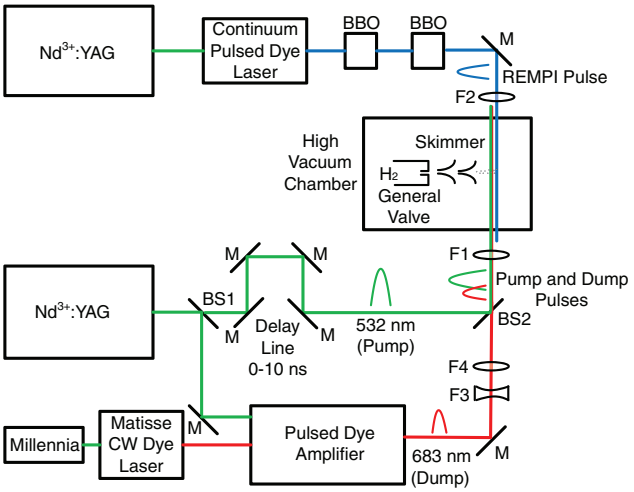

FIG. 1. Schematic of the SARP experiment: M = mirror, F = lens, BS = beam splitter, and BBO = β-barium borate crystal. A multichannel plate ion detector is at right angles to the REMPI pulse path and is not shown.

the dump laser pulse at the dichroic beam splitter (BS2). Using a beam expander on the dump optical path, we can control the focus of the dump pulse in the excitation region as well as compensate for chromatic aberration using a single convex lens. With the help of a Spiricon laser beam profiler (Ophir Optronics), the focuses of the pump and dump laser beams were brought together within the vacuum chamber by adjusting the distance between the concave (F3) and convex (F4) lenses of the beam expander. The two focuses do not necessarily coincide with the center of the molecular beam. Using a 400 mm focal length lens (F1) in front of the vacuum chamber (see Fig. 1), the intensity full width at half maximum (FWHM) of the pump and dump laser beams at the focus were measured to be 30 μm × 38 μm (with the major axis in the horizontal direction) and 20 μm × 20 μm, respectively.

The delay between the pump and dump pulses were calibrated using a fast photodiode (Electro-Optics Technology, ET-2000) on a fast Tektronix (DPO4102B-L) oscilloscope. The pump and dump laser pulses are approximately Gaussian in shape with a duration (intensity FWHM) of 6 ns and 4.6 ns, respectively.

For the Q(0) transition, the pump laser frequency is held fixed at 563270.5 GHz, while the dump laser frequency is varied near 438523.5 GHz. The dump laser frequency which maximizes population transfer depended on the inter-pulse delay and fluence of the pump and dump pulses. The H_2 molecular beam generated from a Series 99 General Valve is skimmed twice before intersecting at right angles to the collinear pump and dump laser pulses. The pulsed valve is mounted on a translation stage which could be adjusted to position the H_2 molecular beam relative to the focus of the pump and dump laser beams. The diameter of the molecular beam in the excitation zone has an intensity FWHM of 1 mm. The energies of the single-mode pump and dump laser pulses were measured 200 mJ and 20 mJ outside the vacuum chamber before the focusing lens. The ground and excited H_2 molecules are state-specifically detected by means of a 2 + 1 resonance enhanced multiphoton ionization (REMPI) scheme, using the $H_2E, F^1\Sigma_g^+(v' = 0, J' = J) - X^1\Sigma_g^+(v = 0, 1, J)$ transition.[21,22] The REMPI UV laser beam counterpropagates along the pump and dump laser beams and is focused on the molecular beam using a ~20 cm focal length lens (F2). The resulting H_2^+ molecules are extracted and accelerated to the multichannel plate (MCP) detector by a dual-stage Wiley-McLaren linear time-of-flight mass spectrometer.

III. RESULTS AND DISCUSSION

Figure 2 shows the H_2 (v = 0, J = 0) and the H_2 (v = 1, J = 0) REMPI signal intensities as a function of detuning. The field-free resonance (i.e., in the absence of the laser pulses) is defined by $\omega_{10} = \omega_P - \omega_D$, where ω_{10} is the frequency difference between the H_2 (v = 0, J = 0) and H_2 (v = 1, J = 0) energy levels of the ground electronic state, and ω_P and ω_D are the angular frequencies of the pump and dump laser pulses. The frequency of the UV laser beam is adjusted to maximize the two-photon REMPI transition for each level (v = 0, J = 0 and v = 1, J = 0). The frequency of the dump laser ω'_D is scanned at a rate of 12.5 MHz/step by controlling the voltage applied to the scan piezo of the Mattise dye laser. The detuning δ is defined as $\delta = \omega'_D - \omega_D$. To avoid the AC Stark shift of the 2 + 1 REMPI signal, the REMPI UV pulse is delayed by 20 ns relative to the dump laser pulse. 2 + 1 REMPI signals from the excited H_2 (v = 1, J = 0) and ground H_2 (v = 0, J = 0) are recorded as a function of δ. At each step of the frequency scan, REMPI signals from 20 laser pulses were averaged to acquire one data point.

An unambiguous measure of population transfer relies on detecting the depletion of the H_2 (v = 0, J = 0) REMPI signal

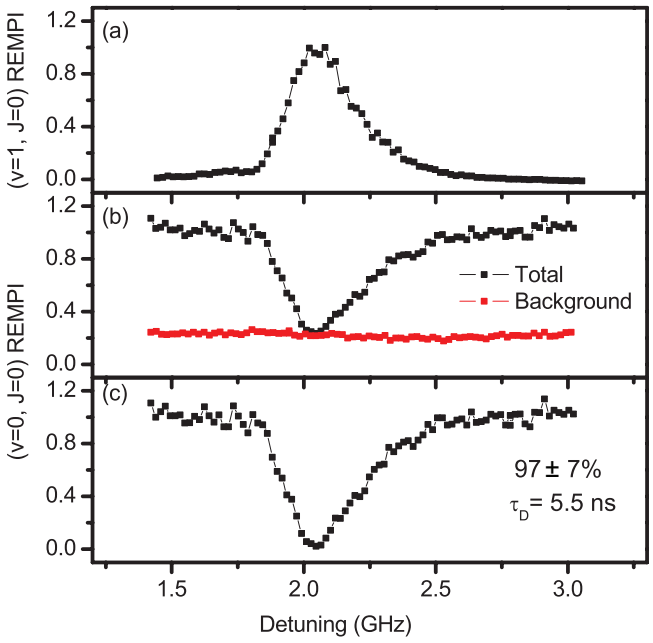

FIG. 2. The (2 + 1) REMPI signal intensities (arbitrary units) of the $H_2E, F^1\Sigma_g^+(v' = 0, J' = J) - X^1\Sigma_g^+(v = 0, 1, J)$ transitions versus the dump laser frequency detuning at a delay of 5.5 ns between the pump and dump laser pulses: (a) The (2 + 1) REMPI signal from H_2 (v = 1, J = 0); (b) from H_2 (v = 0, J = 0) with both background and molecular beam (black dots) and only the background (red dots); and (c) from H_2 (v = 0, J = 0) molecular beam with the background removed by subtraction.

caused by SARP population transfer to the H_2 ($v = 1$, $J = 0$) excited state. Because the H_2 molecules in the molecular beam have the speed ~2500 m/s, during the 20 ns delay between pumping and probing, the excited H_2 molecules move an average distance of ~50 μm along the beam. In order to make sure molecules in the probe region are all from the excitation region, the REMPI laser pulse is focused slightly downstream of the molecular beam relative to the SARP excitation region. The optimum position of the REMPI beam is adjusted by maximizing the REMPI depletion signal from H_2 ($v = 0, J = 0$).

Figure 2(a) shows the H_2 ($v = 1, J = 0$) REMPI signals versus the detuning δ of the dump laser. When the detuning is large, no H_2^+ is detected. This clearly shows that there is no off-resonant pumping of H_2 ($v = 1, J = 0$) and there is no off-resonant multiphoton ionization of H_2 ($v = 0, J = 0$) molecules. The actual position of the peak is determined by the SARP dynamics as explained later.

Because of the poor pumping of H_2 molecules in our vacuum chamber, there is a constant H_2 ($v = 0, J = 0$) background in the excitation region. The background H_2 ($v = 0, J = 0$) molecules move in random directions with a Boltzmann velocity distribution. Although SARP is able to uniformly pump the background H_2 ($v = 0, J = 0$) in the excitation region, our detection process, which relies on detecting molecules downstream, will have a contribution from the H_2 ($v = 0, J = 0$) background. To correctly determine the population transfer we must eliminate the isotropic background and extract the contribution from the molecular beam. This is accomplished in the following way. We first obtain one set of data that have the depletion from both the molecular beam and the background (Fig. 2(b), black dots), and then we physically move the molecular beam ~1 cm away from the laser excitation region by using the translation stage attached to the pulsed valve holder and collect the depletion from the background (Fig. 2(b), red dots). After subtracting the second set of data from the first, we obtain the depletion of H_2 ($v = 0$, $J = 0$) molecules in the molecular beam (Fig. 2(c)) caused by SARP. Following the background subtraction, we find that 97% ± 7% of H_2 ($v = 0, J = 0$) molecules in the molecular beam have been transferred to the H_2 ($v = 1, J = 0$) level by the SARP process, that is, we are able to achieve nearly complete population transfer from the ($v = 0, J = 0$) to ($v = 1, J = 0$) level. The 7% uncertainty estimate is based on the propagation of errors arising from fluctuations in the two REMPI signals shown in Fig. 2(b). The relatively large error bars in the fractional population transferred is caused by H_2 background in the vacuum chamber, which has not been pumped away between molecular beam pulses. Clearly, a vacuum chamber with differential pumping would significantly reduce this background. Note that the FWHM and the peak positions of Figs. 2(a)–2(c) match each other, as expected.

Figure 3 shows the depletion of H_2 ($v = 0, J = 0$) REMPI signal as a function of the dump detuning for different time delays, 0 ns, 3 ns, 5.5 ns, and 9 ns, between the pump and dump laser pulses. In this experiment, the pump laser pulse is followed by a relatively weaker (nine times less fluence) dump laser pulse. Although the exact fluences used to optimize population transfer cannot be directly measured, an estimate can be obtained from theoretical simulations, shown in Fig. 4. Analysis suggests pump fluences in the range of 60–90 J/cm^2 for the delays of 0, 3, and 5.5 ns and a pump to dump fluence ratio of 9. For the 9 ns delay, the simulation suggests that the pump fluence is nearly doubled.

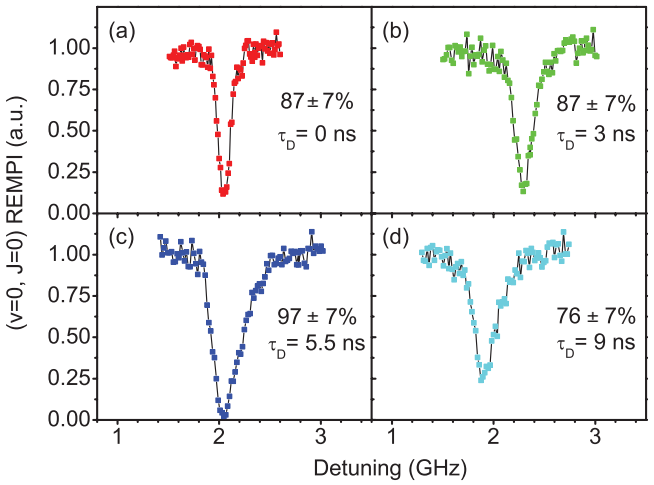

FIG. 3. 2 + 1 REMPI signal for the H_2 $H_2E, F^1\Sigma_g^+(v' = 0, J' = J) - X^1\Sigma_g^+(v = 0, J)$ transition versus the dump laser frequency detuning after the background subtraction for different time delays between the pump and the dump laser pulses: (a) 0 ns; (b) 3 ns; (c) 5.5 ns; and (d) 9 ns.

From Fig. 3, we obtain four important pieces of information. First, the extent of H_2 ($v = 0, J = 0$) depletion is not the same for the four different time delays; the depletion maximizes for a delay of 5.5 ns. Second, the peak widths are different for the four delays. The FWHM of the peak first increases with increasing delay, maximizes at 5.5 ns, and then narrows as the delay increases further. Third, the location of peak frequency shifts with the delays. Finally, for all four different time delays we achieved more than 70% population transfer, which indicates that SARP is a robust technique.

Figure 4 shows a theoretical simulation of the H_2 ($v = 0$, $J = 0$) fractional population as a function of the dump laser frequency for the four delays of 0 ns, 3 ns, 5.5 ns, and 9 ns. Although the peak widths are closely matched to the experimental results shown in Fig. 3, the calculated depletion

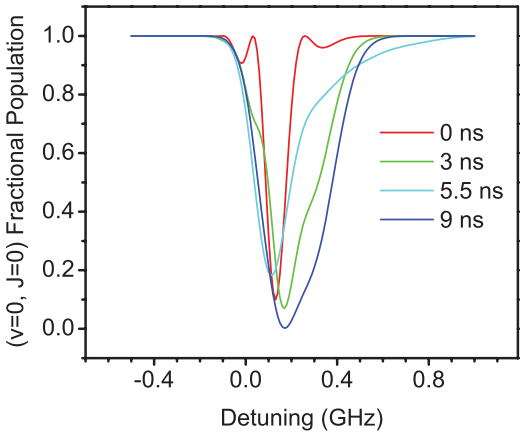

FIG. 4. Theoretical calculation of the H_2 ($v = 0, J = 0$) fractional population versus the dump laser frequency detuning, for the same experimental conditions as presented in Fig. 3.

at the same delay is somewhat larger, especially for the 0 ns, 3 ns, and 9 ns delays for which the peak widths are relatively narrow. In agreement with the experimental data shown in Fig. 3, the theoretical plots in Fig. 4 show the same trend that the FWHM of the depletion peak first increases with delay, maximizes at 5.5 ns, and then decreases at longer time delays. The small relative shifts of the peak positions found in the theoretical calculation cannot be matched with the experimental observation, because the finite accuracy of our wavemeter does not allow us to locate the absolute peak position of the depletion.

In what follows we explain the dynamics of SARP process for different time delays between the pump and dump laser pulses. Figure 5 shows a theoretical simulation of the temporal dynamics of SARP for a given dump laser frequency and pump to dump delay of 5.5 ns. Figure 5(a) presents the intensity profiles of the pump and dump laser pulses and Fig. 5(b) presents the time evolution of the Rabi frequency r, which is proportional to the product of the electrical fields of the pump and the dump laser pulses, $r \propto E_P E_D^*$. The time zero corresponds to peak intensity of the pump laser pulse. Figure 5(c) shows the Stark shifted H_2 ($v = 0$, $J = 0$) and the H_2 ($v = 1$, $J = 0$) energy levels. Based on the data provided in Ref. 23, the magnitudes of the Stark shifts for these two levels are calculated. In the left side of Fig. 5(c), ω_{10} is the field-free Raman transition frequency between the unshifted

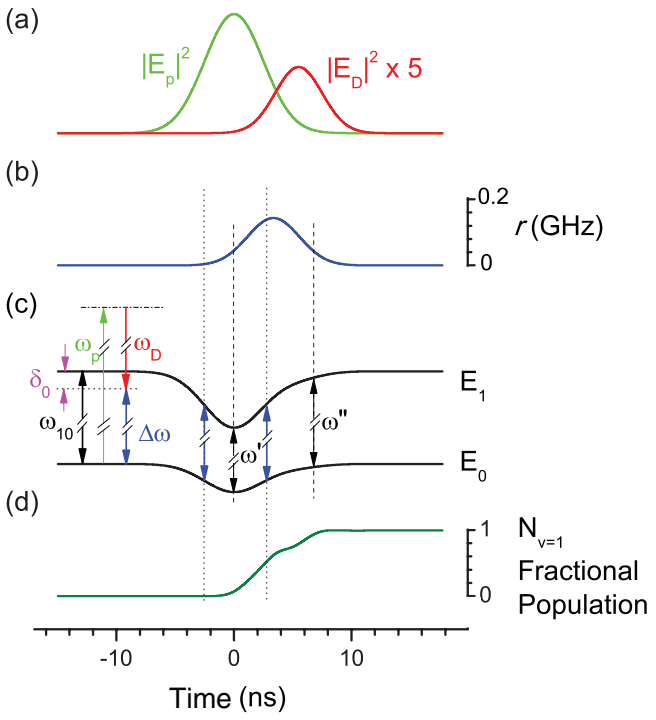

FIG. 5. Calculated SARP pumping process as a function of time for the dump laser pulse delayed by 5.5 ns relative to the pump laser pulse: (a) the evolution of the pump and dump laser pulses with electric fields E_P and E_D; (b) the Rabi frequency r, (c) the Stark-shifted energy levels E_0 and E_1 for the H_2 ($v = 0$, $J = 0$) and the H_2 ($v = 1$, $J = 0$) levels, and (d) the fractional population transferred from the H_2 ($v = 0$, $J = 0$) to H_2 ($v = 1$, $J = 0$). The two dotted vertical lines indicate the positions of the first and second dynamic resonance conditions, and the two dashed lines indicate the positions where the Rabi frequency r reaches a threshold value.

energy levels E_1 and E_0. Here ω_P and ω_D are the angular frequencies of the pump and dump laser pulses, respectively. We define $\Delta\omega = \omega_P - \omega_D$ and $\delta_0 = \Delta\omega - \omega_{10}$. The dynamic Raman resonance condition is satisfied whenever the detuning is compensated by the laser-induced Stark shifts of the energy levels E_1 and E_0. Figure 5(d) shows the fractional population of H_2 ($v = 0$, $J = 0$).

At some time during the rise of the pump pulse intensity, the dynamic Raman resonance condition ($\Delta\omega = E_1 - E_0/\hbar$) is satisfied. This is the first crossing of the resonance during which the Rabi frequency r is too weak to transfer any population to the excited state, which is shown by the left most dotted vertical line in Fig. 5(c). As the Rabi frequency r increases with time, population begins to be transferred to the excited state. However, to transfer population to the excited state at the end of the pulsed excitation, the Raman resonance must be crossed in the presence of a sufficiently strong Rabi frequency r. This condition of adiabatic passage is satisfied at the second resonance crossing, indicated by the right most dotted vertical line in Fig. 5(c). The complete population transfer takes place at the end of the laser pulses, as shown in Fig. 5(d).

Using Fig. 5 we can also explain the origin of the spectral width. As we vary the dump laser frequency ω_D for given fluences of the pump and dump laser pulses, the crossing time of the dynamic resonance shifts. For example, with an increasing value of the initial detuning δ_0, we require a larger Stark shift brought about by higher pump intensity. This condition moves the resonance crossing closer to the peak of the pump laser pulse and away from the time at which the Rabi frequency r reaches its peak as seen in Fig. 5(c). The adiabatic passage of population, however, requires that the Rabi frequency r be above a threshold, which in this case is ~0.044 GHz, during the crossing of the second resonance in Fig. 5. At the two limits where $\Delta\omega$ becomes equal to ω' or ω'', indicated by the two dashed lines in Fig. 5(c), the Rabi-frequency satisfies the threshold condition for adiabatic passage. The spread between ω' and ω'' determines the FWHM of the depletion peak.

For given values of the fluences and delay, the peak position of SARP spectrum is also determined by the condition of adiabatic passage, namely, the Rabi frequency must satisfy the threshold condition. If the resonance is crossed near the peak value of r for a given value of $\Delta\omega$, then maximum population transfer occurs.

Figure 6 shows the SARP temporal dynamics for a delay of 9 ns between the pump and dump laser pulses. For large delay, the peak of the Rabi frequency r appears near the tail of the pump pulse where the intensity has fallen (Figs. 6(a) and 6(b)). In order to cross the resonance adiabatically with sufficiently strong Rabi frequency r, we therefore need a small initial detuning (approximately −0.1 GHz). For a larger detuning, the resonance crossing will shift closer to the peak of the pump laser pulse and far away from the peak of the Rabi frequency r, causing the condition for adiabatic passage not to be satisfied. In Fig. 6(c), the frequency difference of $\omega'' - \omega'$ gives the spectral width of the depletion peak, which is much narrower than the 5.5 ns condition shown in Fig. 5

Figure 7 shows the pumping process when the pump and dump laser arrives simultaneously in the excitation region.

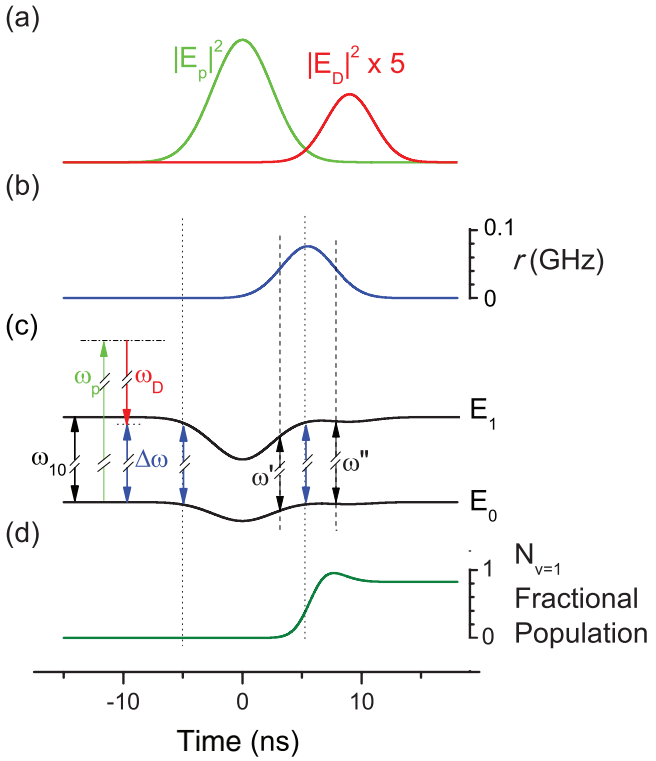

FIG. 6. Calculated SARP pumping process as a function of time for the dump laser pulse delayed by 9 ns relative to the pump laser pulse. All symbols are the same as defined in the caption to Fig. 5.

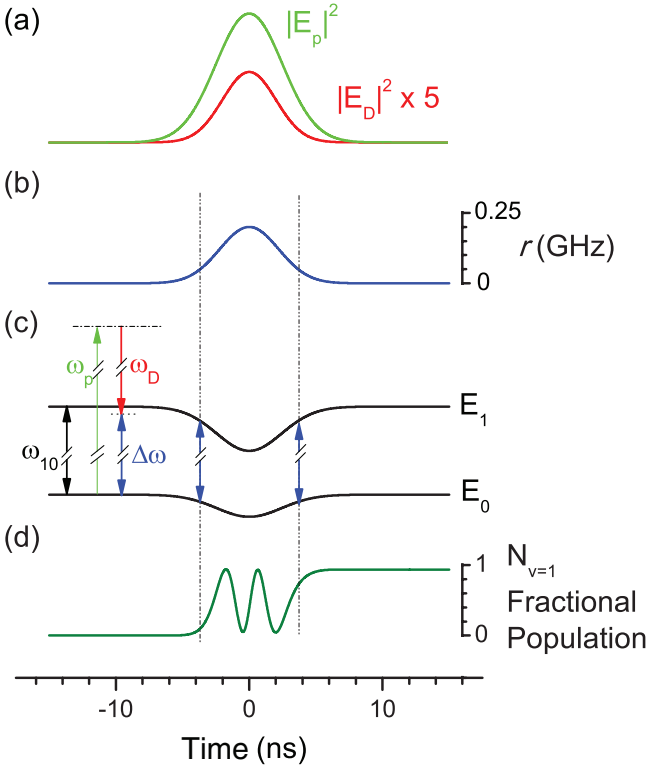

FIG. 7. Calculated SARP pumping process as a function of time for the pump and dump laser pulses arriving simultaneously. All symbols are the same as defined in the caption to Fig. 5.

For this case, the Rabi frequency is equally strong at both crossings. If the adiabatic passage condition is obeyed, we obtain complete population return at the end of pulsed excitation. Consequently, the only way to avoid the adiabatic passage and to transfer population is by using a sufficiently small Rabi frequency r at both crossings (as indicted by the dashed-dotted lines in Fig. 7). This condition is met using a very small zero-field detuning approximately −0.1 GHz. The limited range of the zero-field detuning required to avoid coherent population return causes the spectral width to be narrow. With the small zero-field detuning, population oscillations, commonly known as the Rabi oscillations, will occur, and population transfer will be extremely sensitive to the fluences and frequencies of the pump and dump laser pulses. It is relatively more difficult to control these laser parameters in practice, although we did achieve approximately 87% ± 7% population transfer (see Fig. 3) by careful tuning of the dump laser frequency.

IV. SUMMARY

Using the Q(0) line of a Raman transition we have demonstrated that SARP can achieve nearly complete population transfer (97% ± 7%) from H_2(v = 0, J = 0) to H_2(v = 1, J = 0) state in a beam of H_2 molecules. Of course, under our expansion conditions, the beam contains H_2 molecules in the rotational levels J = 1 and J = 2 that are not pumped. The maximum population transfer and the largest spectral width are observed for an inter-pulse delay of 5.5 ns which is comparable to the temporal width of the pump laser pulse. A pump laser pulse fluence of ∼60–90 J/cm^2 and dump laser pulse fluence of ∼7–10 J/cm^2 is estimated by using a theoretical simulation that closely matches with the experimental results. We explored several different SARP conditions and found that in each case we could achieve significant population transfer. We conclude that SARP is a robust and versatile method for preparing quantum states of polar as well as nonpolar isolated molecules which are Raman active. The ability to transfer a large fraction of population to an excited rovibrational level opens new possibilities for studying gas-phase and the gas-surface reactions.

ACKNOWLEDGMENTS

This work was supported by the U.S. Army Research Office under ARO Grant Nos. W911NF-10-1-01318 and W911NF-13-1-0126, a DURIP equipment Grant No. W911NF-11-1-0342, and a MURI Grant No. C13J225+(J00210).

[1]A. Sinha, M. C. Hsiao, and F. F. Crim, J. Chem. Phys. **92**(10), 6333–6335 (1990).
[2]L. B. F. Juurlink, R. R. Smith, D. R. Killelea, and A. L. Utz, Phys. Rev. Lett. **94**(20), 208303 (2005).
[3]S. Yan, Y. T. Wu, B. L. Zhang, X. F. Yue, and K. P. Liu, Science **316**(5832), 1723–1726 (2007).
[4]C. E. Hamilton, J. L. Kinsey, and R. W. Field, Annu. Rev. Phys. Chem. **37**, 493–524 (1986).
[5]X. Yang, J. M. Price, J. A. Mack, C. G. Morgan, C. A. Rogaski, D. Mcguire, E. H. Kim, and A. M. Wodtke, J. Phys. Chem. **97**(16), 3944–3955 (1993).

[6]U. Gaubatz, P. Rudecki, S. Schiemann, and K. Bergmann, J. Chem. Phys. **92**(9), 5363–5376 (1990).
[7]G. Z. He, A. Kuhn, S. Schiemann, and K. Bergmann, J. Opt. Soc. Am. B **7**(9), 1960–1969 (1990).
[8]U. Gaubatz, P. Rudecki, M. Becker, S. Schiemann, M. Kulz, and K. Bergmann, Chem. Phys. Lett. **149**(5–6), 463–468 (1988).
[9]J. R. Kuklinski, U. Gaubatz, F. T. Hioe, and K. Bergmann, Phys. Rev. A **40**(11), 6741–6744 (1989).
[10]M. Oberst, H. Munch and T. Halfmann, Phys. Rev. Lett. **99**(17), 173001 (2007).
[11]M. Oberst, H. Muench, G. Grigoryan, and T. Halfmann, Phys. Rev. A **78**(3), 033409 (2008).
[12]L. P. Yatsenko, S. Guerin, and H. R. Jauslin, Phys. Rev. A **65**(4), 043407 (2002).
[13]T. Rickes, L. P. Yatsenko, S. Steuerwald, T. Halfmann, B. W. Shore, N. V. Vitanov, and K. Bergmann, J. Chem. Phys. **113**(2), 534–546 (2000).
[14]N. V. Vitanov, T. Halfmann, B. W. Shore, and K. Bergmann, Annu. Rev. Phys. Chem. **52**, 763–809 (2001).
[15]L. P. Yatsenko, B. W. Shore, T. Halfmann, K. Bergmann, and A. Vardi, Phys. Rev. A **60**(6), R4237–R4240 (1999).
[16]S. Chelkowski and A. D. Bandrauk, J. Raman Spectrosc. **28**(6), 459–466 (1997).
[17]F. Legare, S. Chelkowski, and A. D. Bandrauk, Chem. Phys. Lett. **329**(5–6), 469–476 (2000).
[18]N. Mukherjee and R. N. Zare, J. Chem. Phys. **135**(2), 024201 (2011).
[19]N. Mukherjee and R. N. Zare, J. Chem. Phys. **135**(18), 184202 (2011).
[20]N. Mukherjee, W. R. Dong, J. A. Harrison, and R. N. Zare, J. Chem. Phys. **138**(5), 051101-1–051101-4 (2013).
[21]E. E. Marinero, C. T. Rettner, and R. N. Zare, Phys. Rev. Lett. **48** (19), 1323–1326 (1982).
[22]E. E. Marinero, R. Vasudev, and R. N. Zare, J. Chem. Phys. **78**(2), 692–699 (1983).
[23]M. J. Dyer and W. K. Bischel, Phys. Rev. A **44**(5), 3138–3143 (1991).